

Supplementary information to be published electronically for the paper:

Polypyrrole-Functionalized Ruthenium Carbene Catalysts as Efficient Heterogeneous Systems for Olefin Epoxidation.

Mohamed Dakkach,^{a,b} Xavier Fontrodona,^a Teodor Parella,^c Ahmed Atlamsani,^b Isabel Romero,^{a,*} Montserrat Rodríguez^{a,*}

^a Departament de Química i Serveis Tècnics de Recerca, Universitat de Girona, Campus de Montilivi, E-17071 Girona, Spain. *E-mail:* montse.rodriguez@udg.edu, marisa.romero@udg.edu.

^b Laboratoire des Matériaux et Systèmes Interfaciaux, Département de Chimie, Faculté des Sciences, B.P.: 2121 93000 Tétouan, Morocco.

^c Departament de Química i Servei de RMN Universitat Autònoma de Barcelona, Cerdanyola del Vallès, E-08193 Barcelona, Spain.

CONTENTS.

Table S 1. Crystal data for the X-ray structures of complexes **2a** and **2b**.

Table S 2. Main bond lengths (Å) and angles (°) for the X-ray structure of complexes **2a** and **2b**.

Figure S 1. Possible diastereoisomers for complex $[\text{Ru}^{\text{II}}\text{Cl}(\text{CN-Me})(\text{bpea-pyr})]^+$, **3**.

Figure S 2. NMR spectra (600 MHz, 298 K, d_6 -acetone) of complex *trans,mer*- $[\text{Ru}^{\text{II}}\text{Cl}_2(\text{bpea-pyr})(\text{dmsO})]$, **2a**: (a) ¹H-NMR, (b) ¹³C-NMR, (c) COSY, (d) NOESY, (e) HSQC, (f) HMBC.

Figure S 3. NMR spectra (600 MHz, 298 K, d_6 -acetone) of complex *cis,fac*- $[\text{Ru}^{\text{II}}\text{Cl}_2(\text{bpea-pyr})(\text{dmsO})]$, **2b**: (a) ¹H-NMR, (b) ¹³C-NMR, (c) COSY, (d) NOESY, (e) HSQC, (f) HMBC.

Figure S 4. NMR spectra (600 MHz, 298 K, d_6 -acetone) *trans,fac*- $[\text{Ru}^{\text{II}}\text{Cl}(\text{CN-Me})(\text{bpea-pyr})]^+$, **3**: (a) ¹H-NMR, (b) ¹³C-NMR, (c) COSY, (d) NOESY, (e) HSQC, (f) HMBC.

Figure S 5. NMR spectra (600 MHz, 298 K, d_6 -acetone) *trans,fac*- $[\text{Ru}^{\text{II}}(\text{CN-Me})(\text{bpea-pyr})(\text{H}_2\text{O})]^{2+}$, **4**: (a) ¹H-NMR, (b) ¹³C-NMR, (c) COSY, (d) NOESY, (e) HSQC, (f) HMBC.

Figure S 6. Cyclic voltammogram of complex **3** (1 mM) registered in CH_2Cl_2 + 0.1 M TBAH at a glassy carbon disk electrode (scan rate = 100 mV s⁻¹).

Figure S 7. Cyclic voltammogram of complex **4** (1 mM) in CH_2Cl_2 + 0.1 M TBAH at a glassy carbon disk electrode (scan rate = 100 mV s⁻¹).

Figure S 8. (a) Growing of a **C/poly-3** film in CH_2Cl_2 + 0.1 M TBAH at a glassy carbon disk electrode (diameter = 3 mm) by scanning the potential between 0 and 1.3 V throughout 30 cycles (scan rate = 100 mV s⁻¹). (b) Cyclic voltammograms registered after transferring the **C/poly-3** modified electrode into a blank electrolyte solution (5 cycles were registered; final amount of anchored complex = $4.36 \cdot 10^{-10}$ mols·cm⁻²).

Figure S 9. Linear regression of $E_{1/2}$ values vs. pH for the cyclic voltammograms of complex **4** registered in aqueous media.

Table S 1. Crystal data for the X-ray structures of complexes **2a** and **2b**.

	Complex 2a	Complex 2b
Chemical formula	C ₂₁ H ₂₈ Cl ₂ N ₄ OSRu	C ₂₁ H ₂₈ Cl ₂ N ₄ OSRu
Molecular weight	556.50	556.50
Crystal system	Monoclinic	Triclinic
Space group	P21/c	P-1
a[Å]	11.0431(5)	9.495(6)
b[Å]	12.1413(6)	15.469(10)
c[Å]	17.3390(8)	16.457(10)
α[°]	90.00	102.506(9)
β[°]	92.3280(10)	90.074(9)
γ[°]	90.00	94.764(10)
V [Å ³]	2322.85(19)	2351(3)
Z	4	4
Temperature, K	300(2)	300(2)
ρ _{calc} , [Mg/m ³]	1.591	1.572
μ[mm ⁻¹]	1.016	1.003
R ₁ ^a [I>2σ(I)]	R ₁ = 0.0257	R ₁ = 0.1806
wR ₂ ^b (all data)	R ₁ = 0.0294 = 0.0694	R ₁ = 0.2396 wR ₂ = 0.4656

$$^a R_1 = \sum ||F_o| - |F_c|| / \sum |F_o|$$

$$^b wR_2 = [\sum \{w(F_o^2 - F_c^2)^2\} / \sum \{w(F_o^2)^2\}]^{1/2}, \text{ where } w = 1/[\sigma^2(F_o^2) + (0.0042P)^2] \text{ and } P = (F_o^2 + 2F_c^2).$$

Table S 2. Main bond lengths (Å) and angles (°) for the X-ray structure of complexes **2a** and **2b**.

Complex 2a		Complex 2b	
Ru(1)-N(1)	2,0685(15)	Ru(1)-N(3)	2,04(2)
Ru(1)-N(3)	2,0859(14)	Ru(1)-N(1)	2,097(16)
Ru(1)-N(2)	2,1656(14)	Ru(1)-N(2)	2,162(15)
Ru(1)-S(1)	2,2321(4)	Ru(1)-S(1)	2,227(6)
Ru(1)-Cl(2)	2,3957(5)	Ru(1)-Cl(1)	2,408(6)
Ru(1)-Cl(1)	2,4550(4)	Ru(1)-Cl(2)	2,439(6)
N(1)-Ru(1)-N(3)	160,82(5)	N(3)-Ru(1)-N(1)	82,9(7)
N(1)-Ru(1)-N(2)	81,16(5)	N(3)-Ru(1)-N(2)	82,6(7)
N(3)-Ru(1)-N(2)	79,78(5)	N(1)-Ru(1)-N(2)	82,1(6)
N(1)-Ru(1)-S(1)	96,22(4)	N(3)-Ru(1)-S(1)	91,3(6)
N(3)-Ru(1)-S(1)	102,95(4)	N(1)-Ru(1)-S(1)	173,9(4)
N(2)-Ru(1)-S(1)	174,82(4)	N(2)-Ru(1)-S(1)	99,0(4)
N(1)-Ru(1)-Cl(2)	90,81(4)	N(3)-Ru(1)-Cl(1)	172,6(6)
N(3)-Ru(1)-Cl(2)	88,16(4)	N(1)-Ru(1)-Cl(1)	91,9(4)
N(2)-Ru(1)-Cl(2)	93,20(4)	N(2)-Ru(1)-Cl(1)	91,6(4)
S(1)-Ru(1)-Cl(2)	91,295(16)	S(1)-Ru(1)-Cl(1)	94,1(2)
N(1)-Ru(1)-Cl(1)	90,81(4)	N(3)-Ru(1)-Cl(2)	96,2(6)
N(3)-Ru(1)-Cl(1)	91,17(4)	N(1)-Ru(1)-Cl(2)	90,8(4)
N(2)-Ru(1)-Cl(1)	89,66(4)	N(2)-Ru(1)-Cl(2)	172,9(4)
S(1)-Ru(1)-Cl(1)	85,903(16)	S(1)-Ru(1)-Cl(2)	88,0(2)
Cl(2)-Ru(1)-Cl(1)	176,900(16)	Cl(1)-Ru(1)-Cl(2)	89,1(2)
O(1)-S(1)-Ru(1)	117,59(6)	O(1)-S(1)-Ru(1)	119,4(8)

Figure S 1. Possible diastereoisomers for complex $[Ru^II Cl(CN-Me)(bpea-pyr)]^+$, 3.

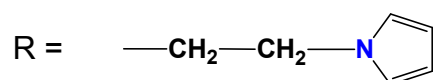
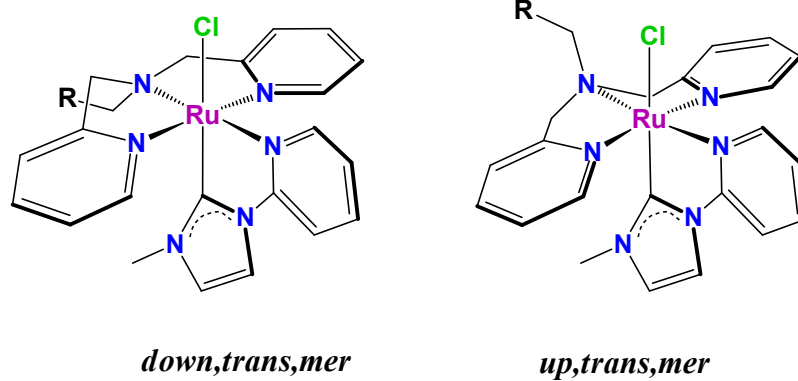
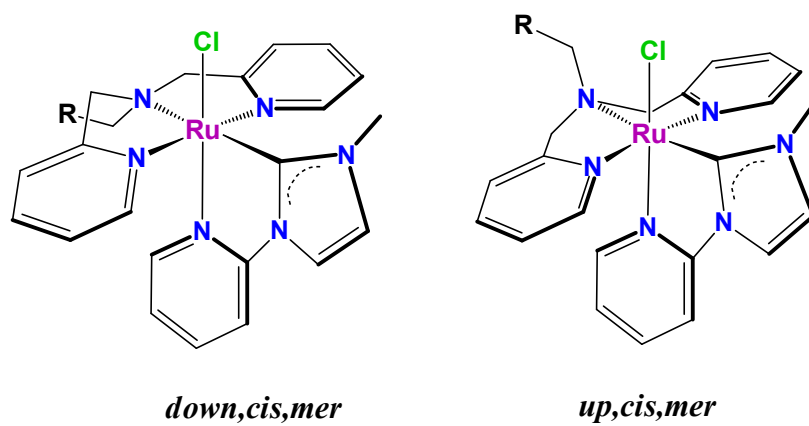
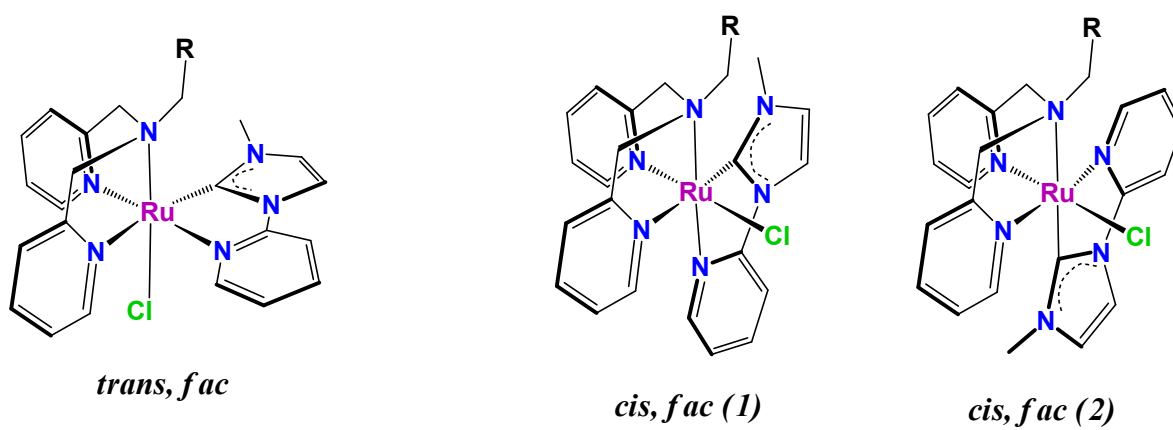
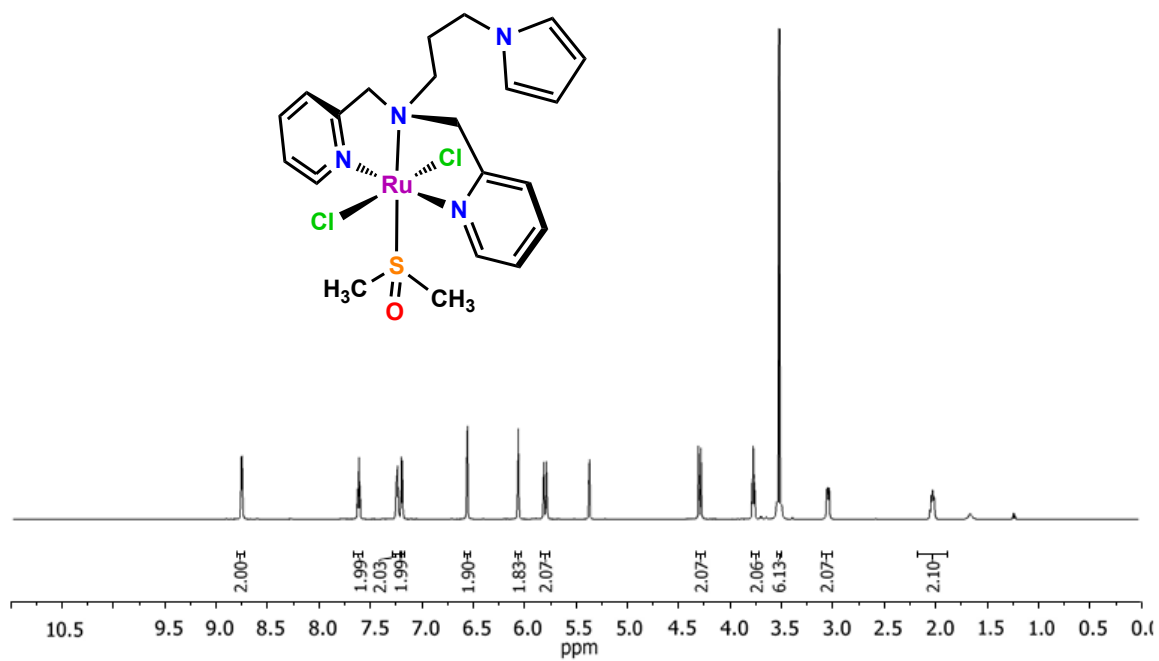
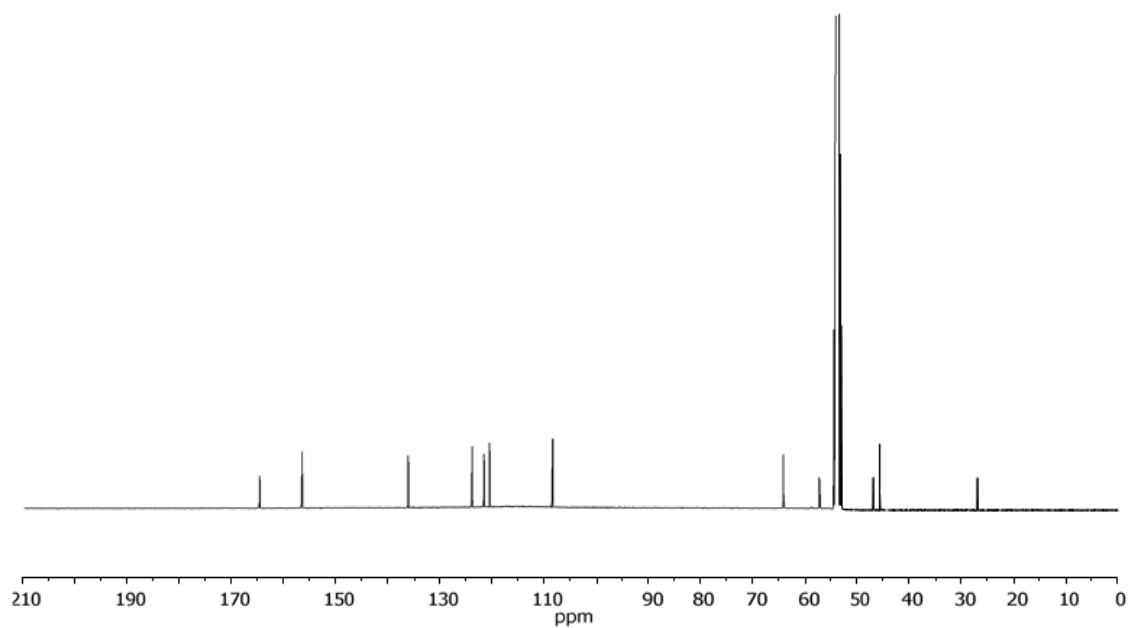


Figure S 2. NMR spectra (600 MHz, 298 K, d_6 -acetone) of complex *trans,mer*-[Ru^{II}Cl₂(bpea-pyr)(dmsc)], **2a**: (a) ¹H-NMR, (b) ¹³C-NMR, (c) COSY, (d) NOESY, (e) HSQC, (f) HMBC.

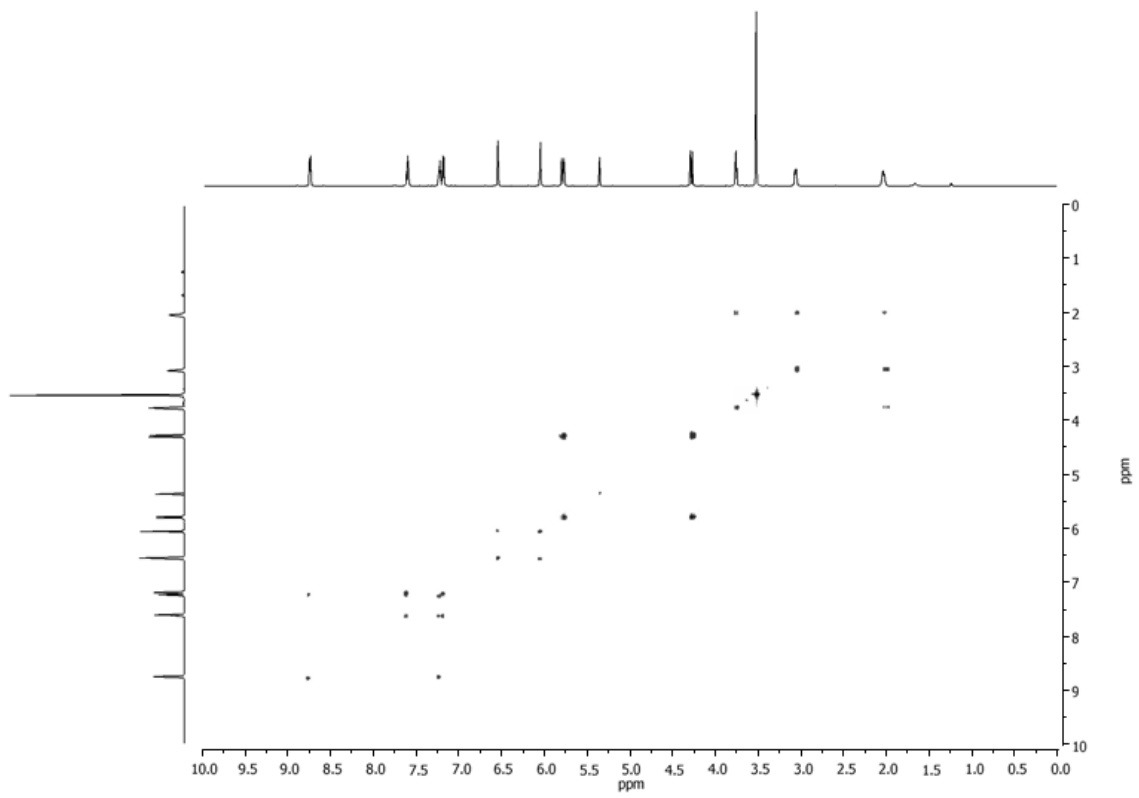
(a)



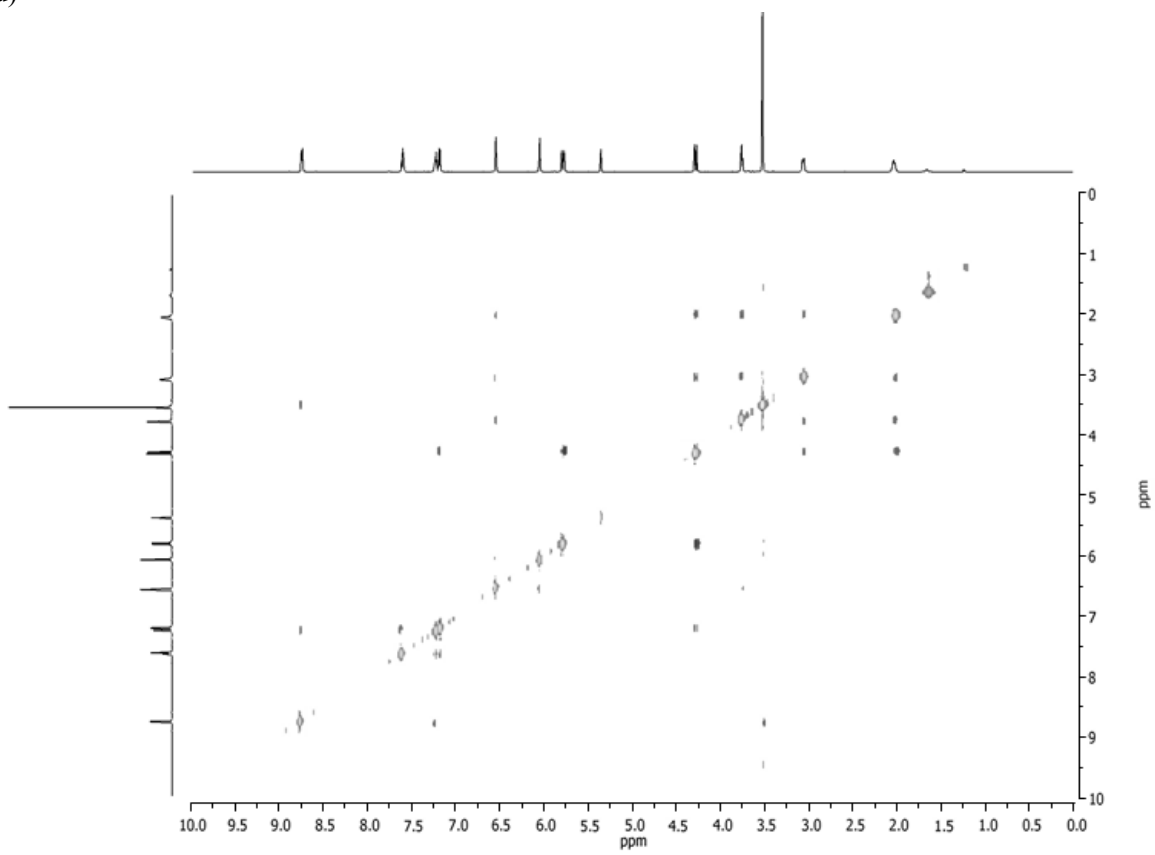
(b)



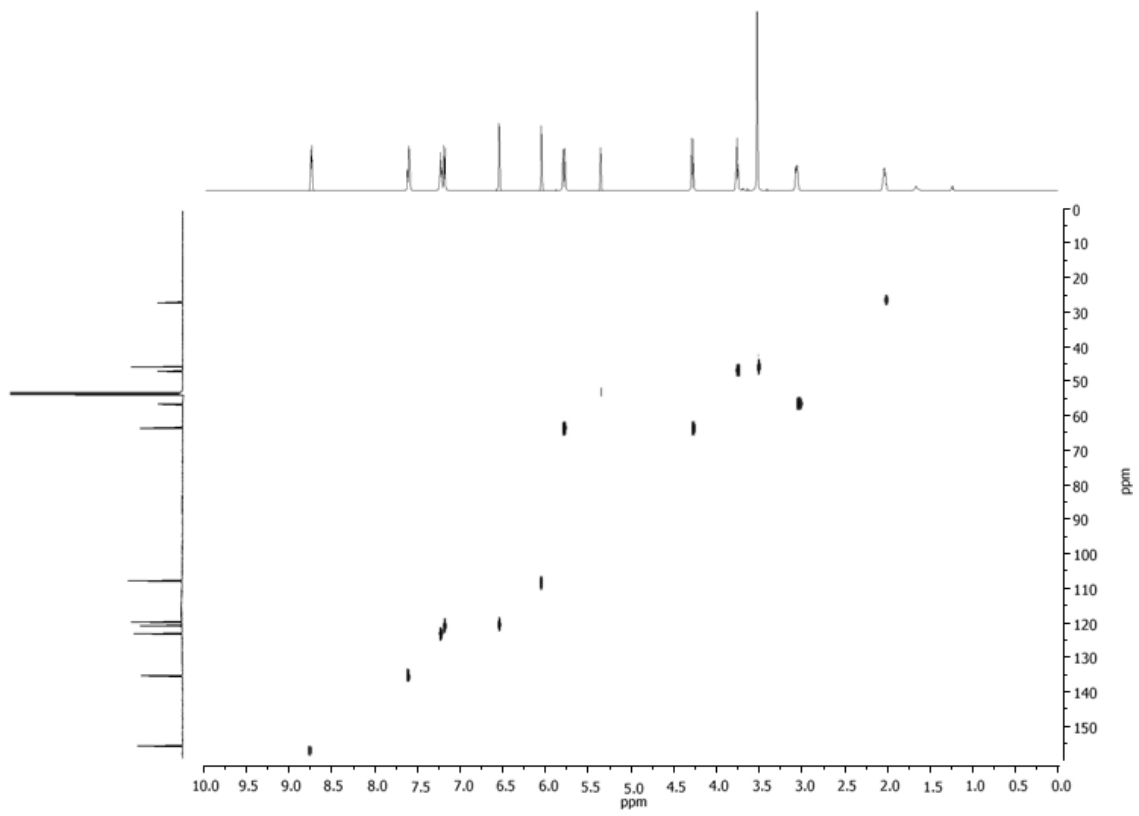
(c)



(d)



(e)



(f)

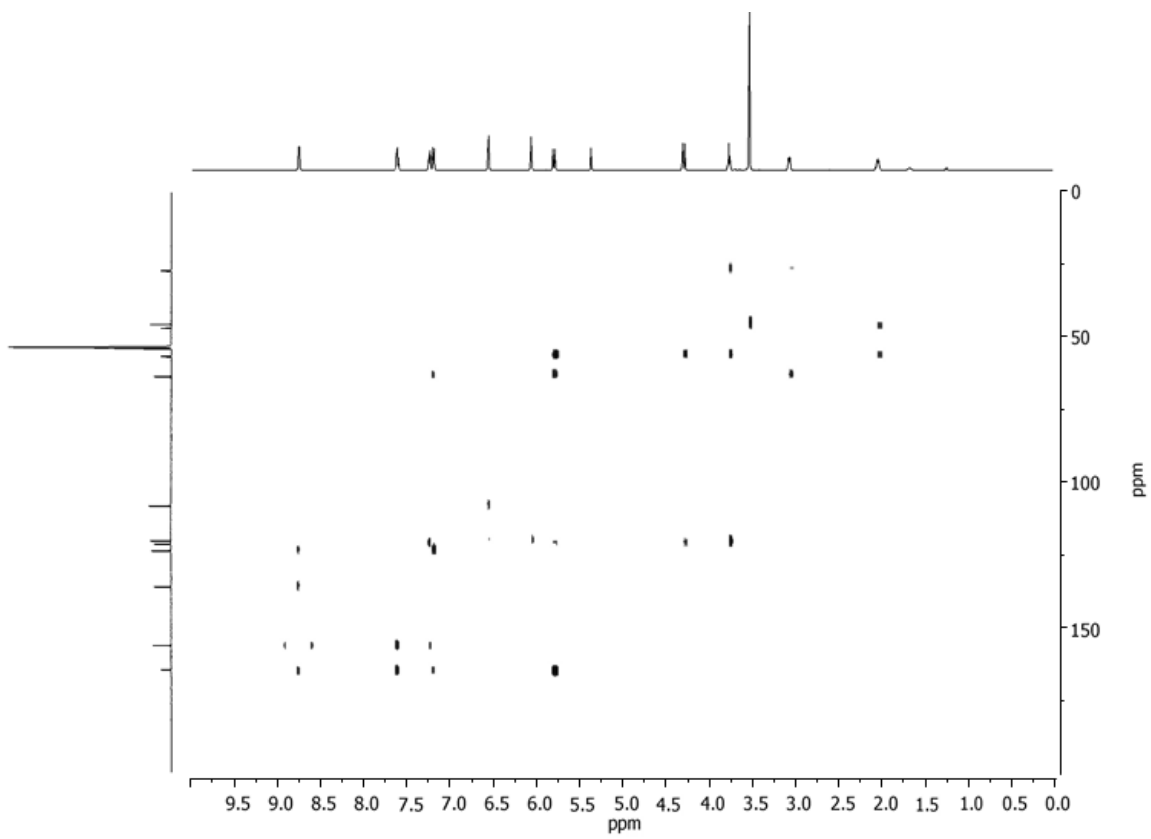
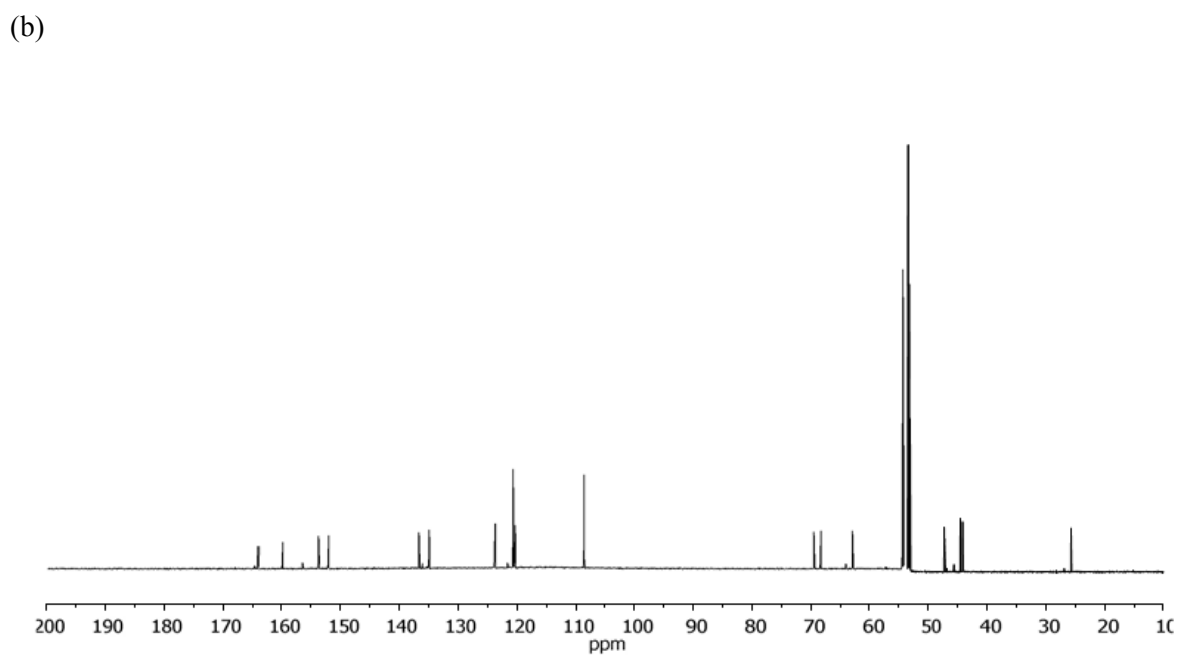
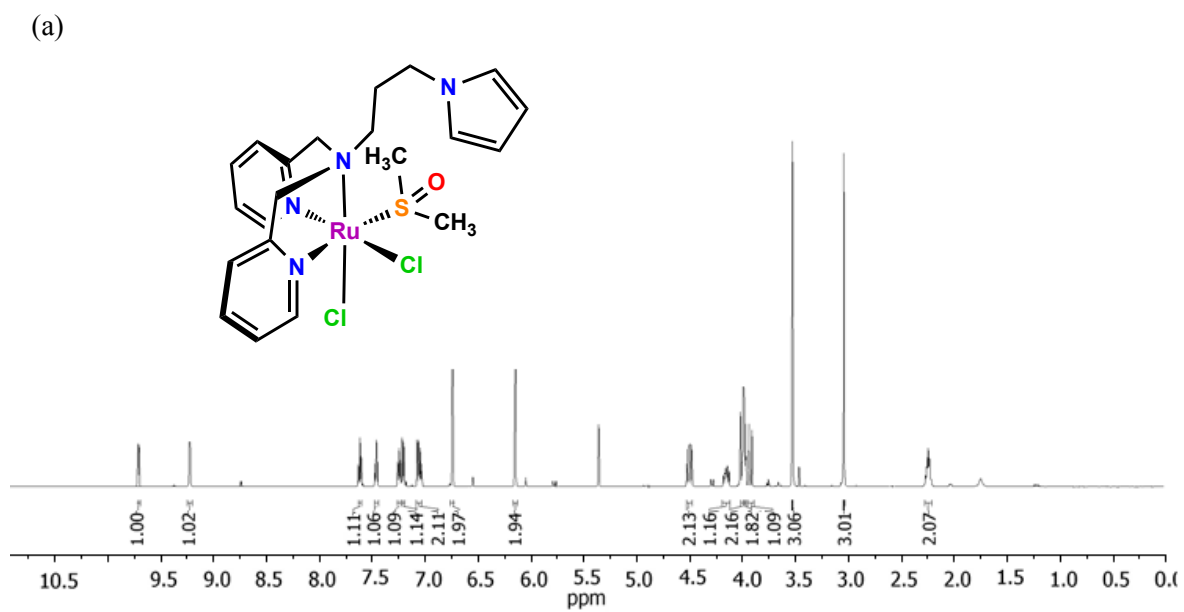
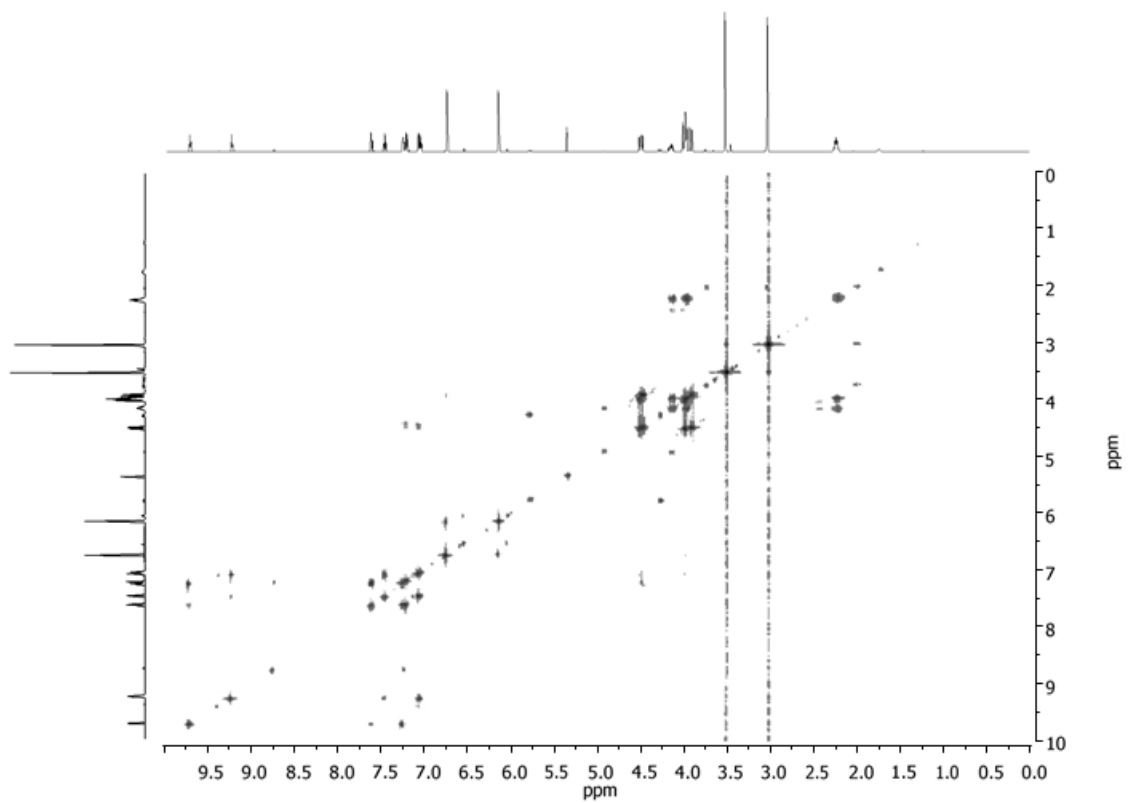


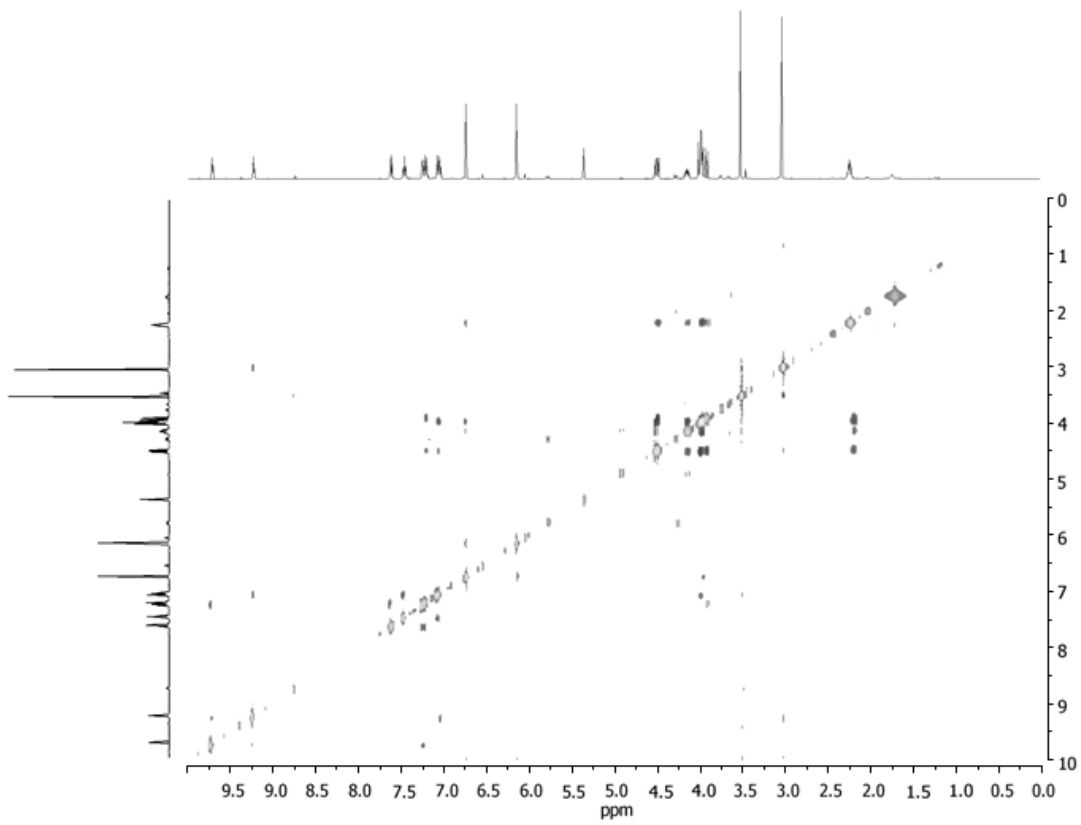
Figure S 3. NMR spectra (600 MHz, 298 K, d_6 -acetone) of complex *cis,trans*-[Ru^{II}Cl₂(bpea-pyr)(dmsc)], **2b**: (a) ¹H-NMR, (b) ¹³C-NMR, (c) COSY, (d) NOESY, (e) HSQC, (f) HMBC.



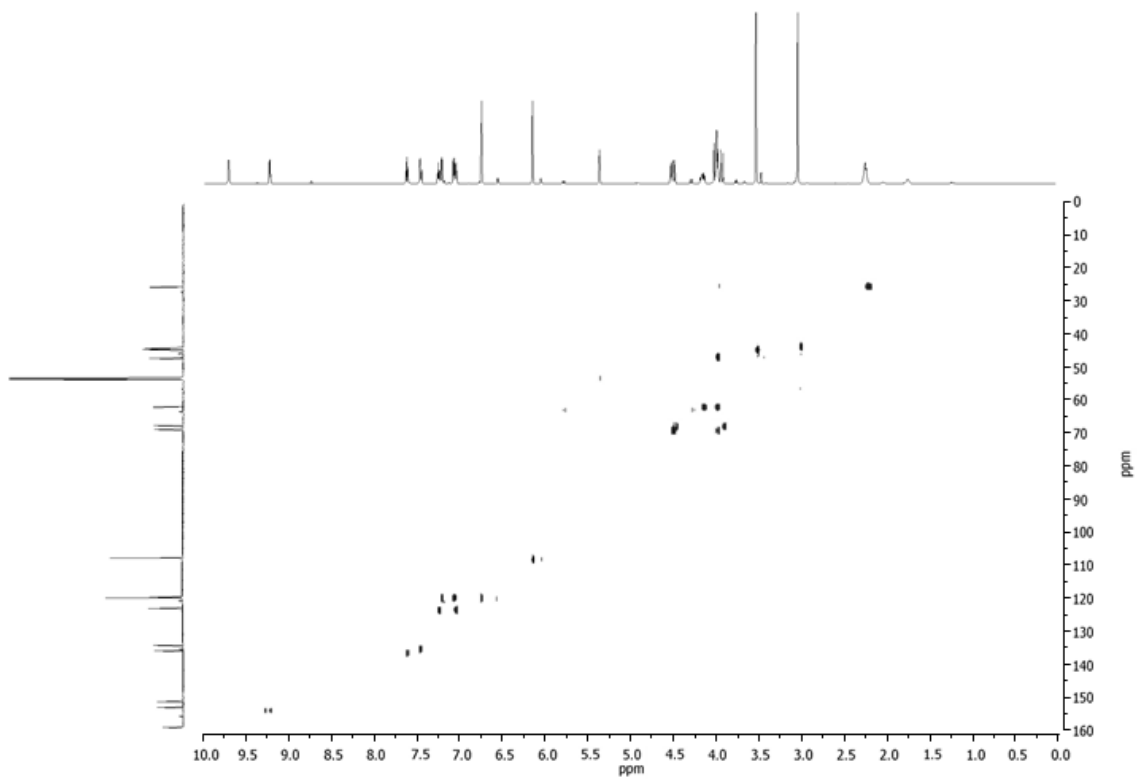
(c)



(d)



(e)



(f)

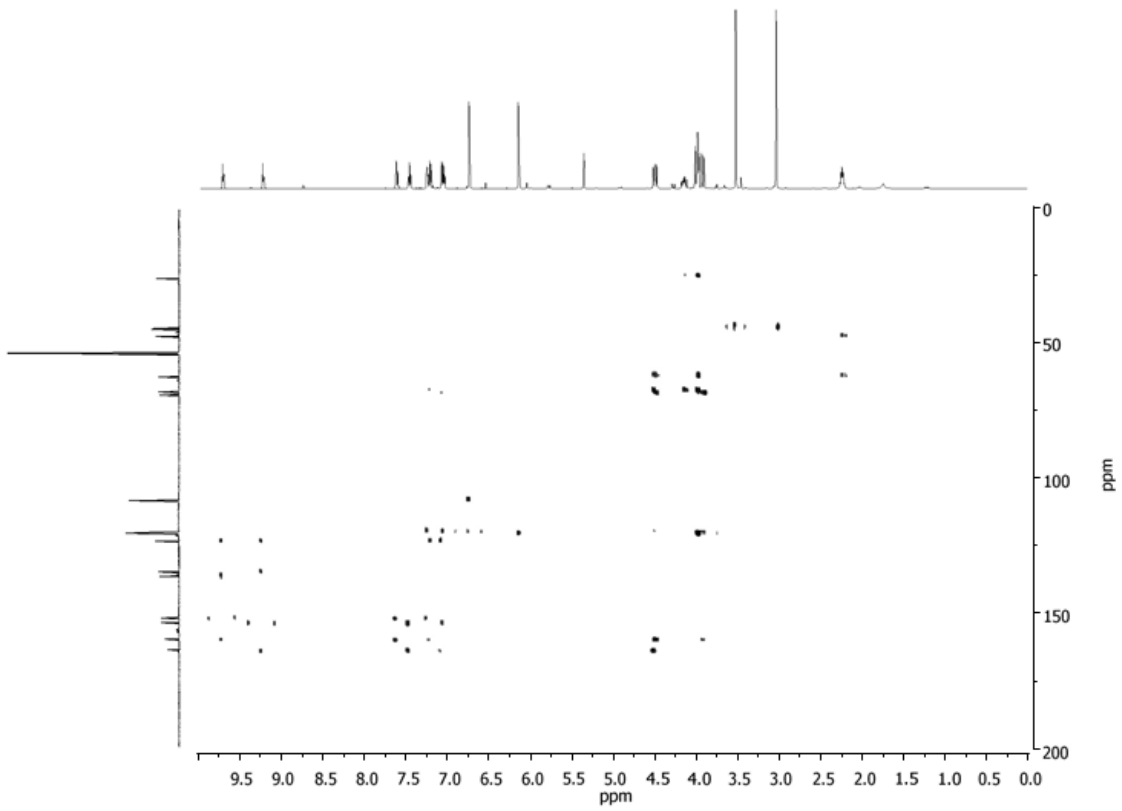
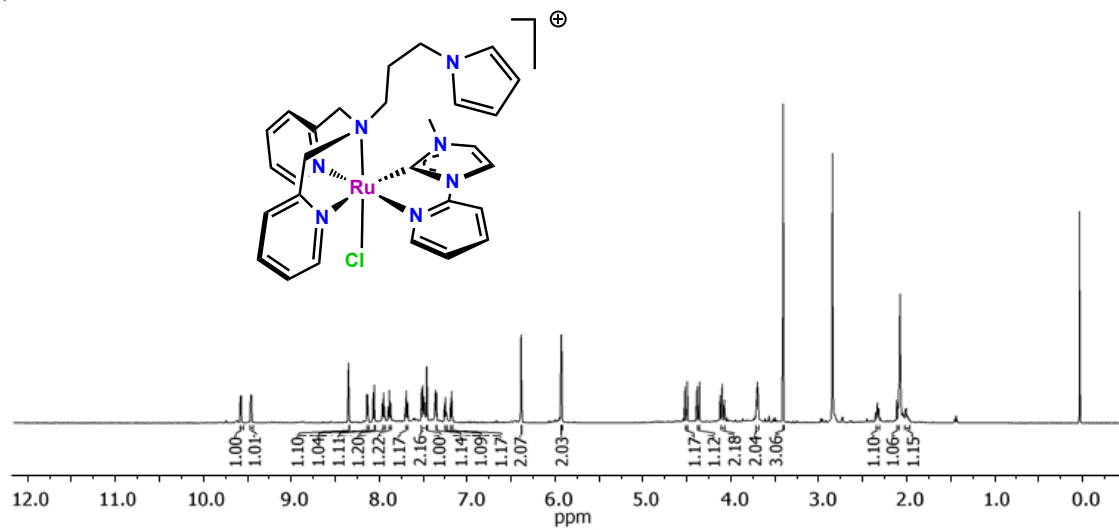
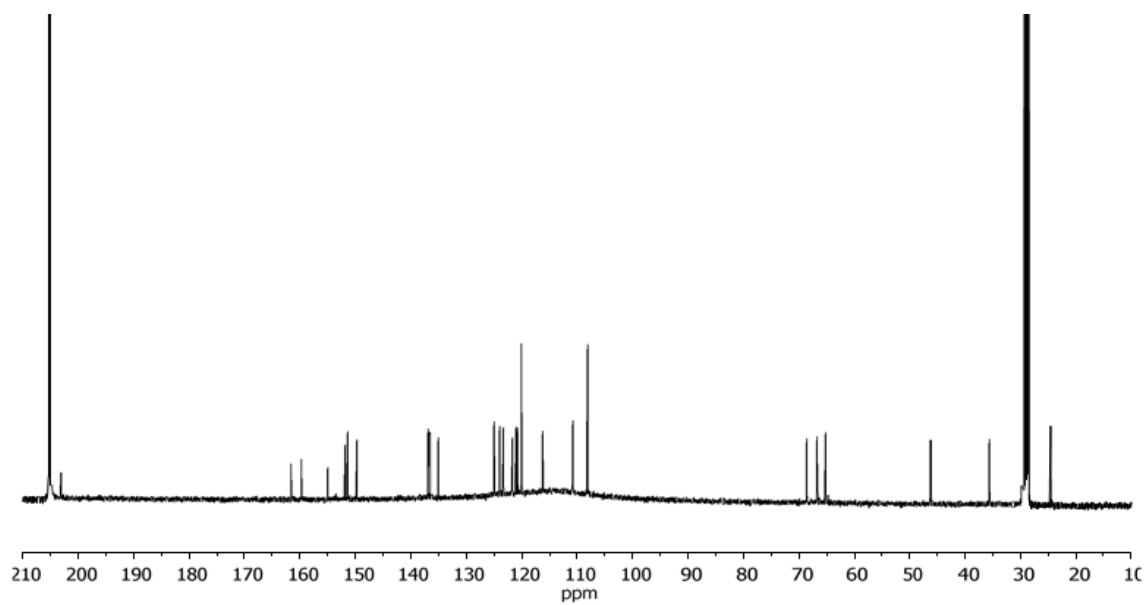


Figure S 4. NMR spectra (600 MHz, 298 K, d_6 -acetone) *trans, fac*-[Ru^{II}Cl(CN-Me)(bpea-pyr)]⁺, **3**: (a) ¹H-NMR, (b) ¹³C-NMR, (c) COSY, (d) NOESY, (e) HSQC, (f) HMBC.

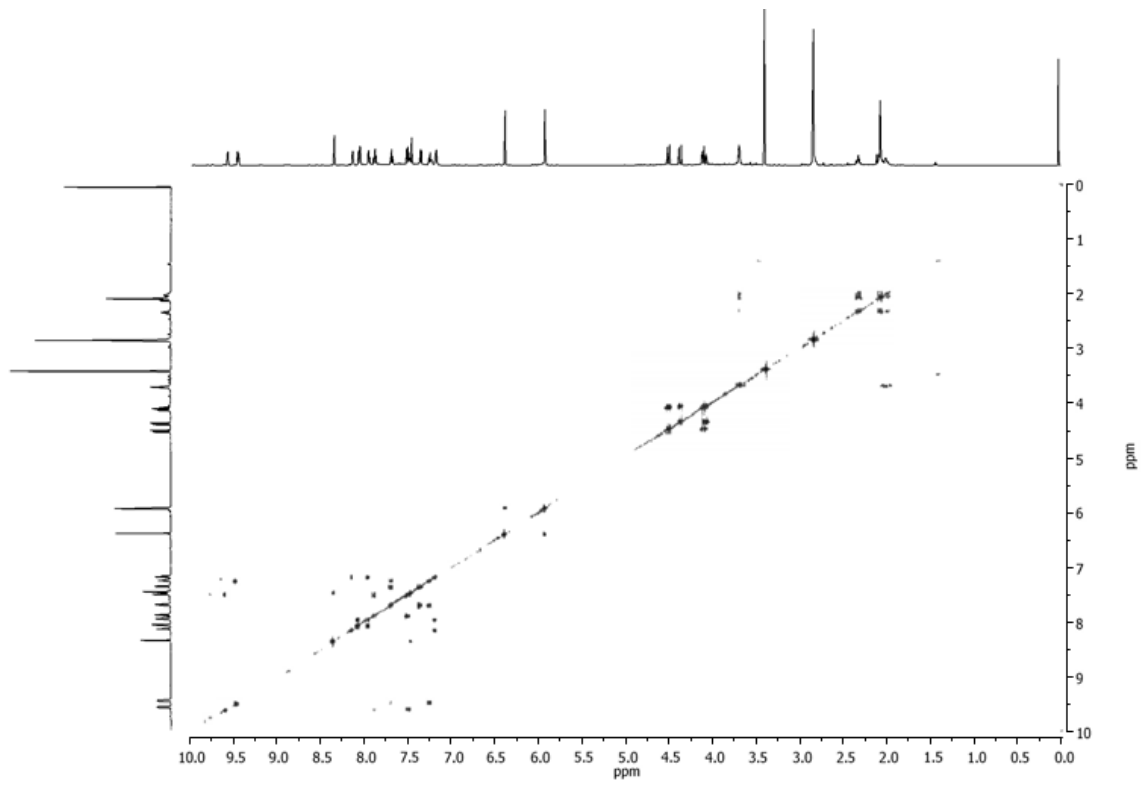
(a)



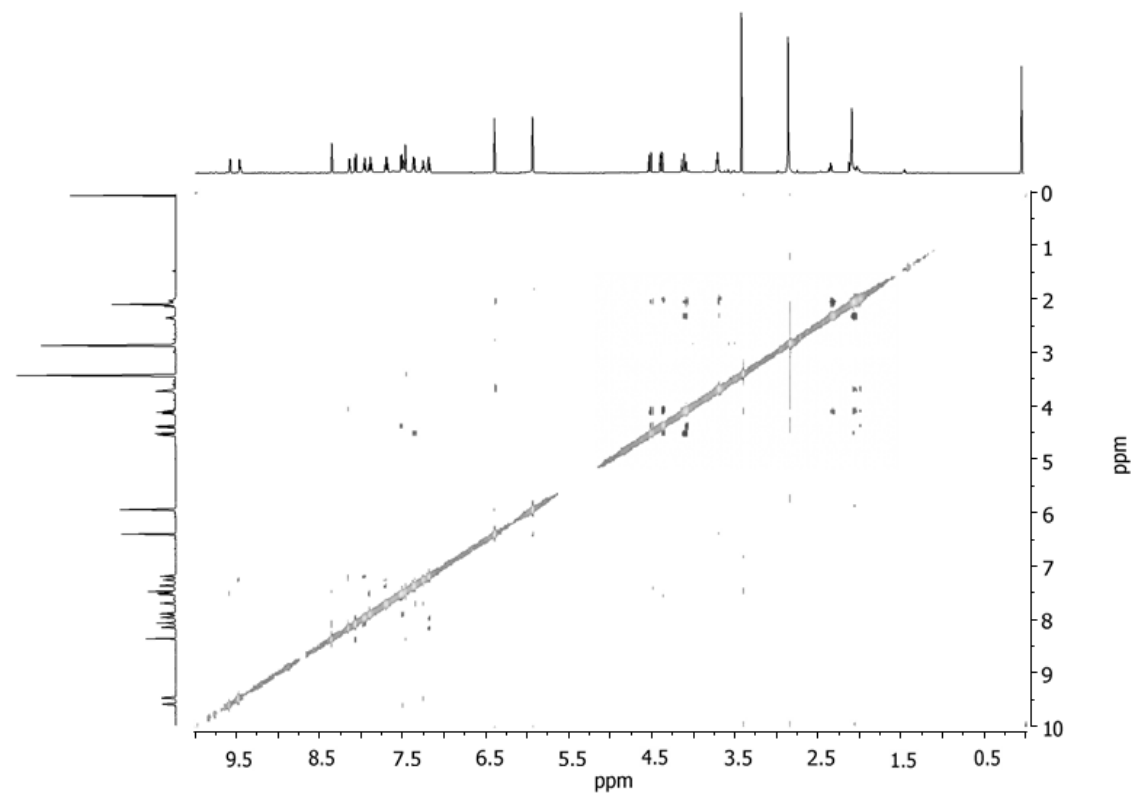
(b)



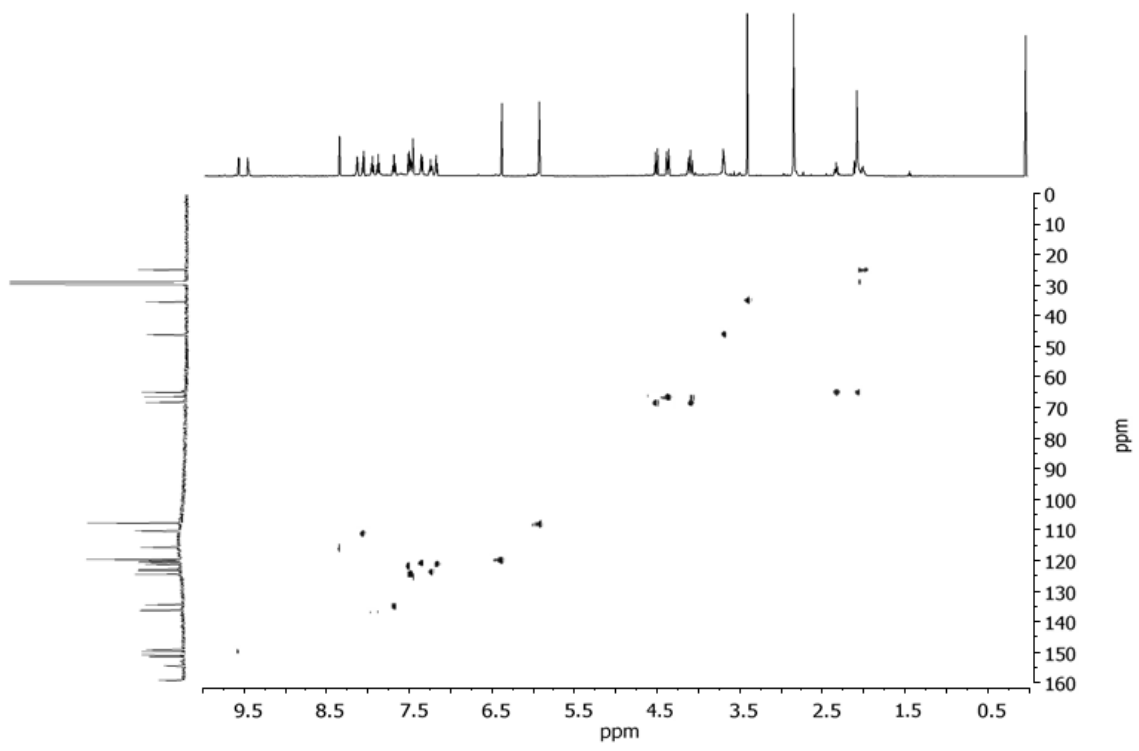
(c)



(d)



(e)



(f)

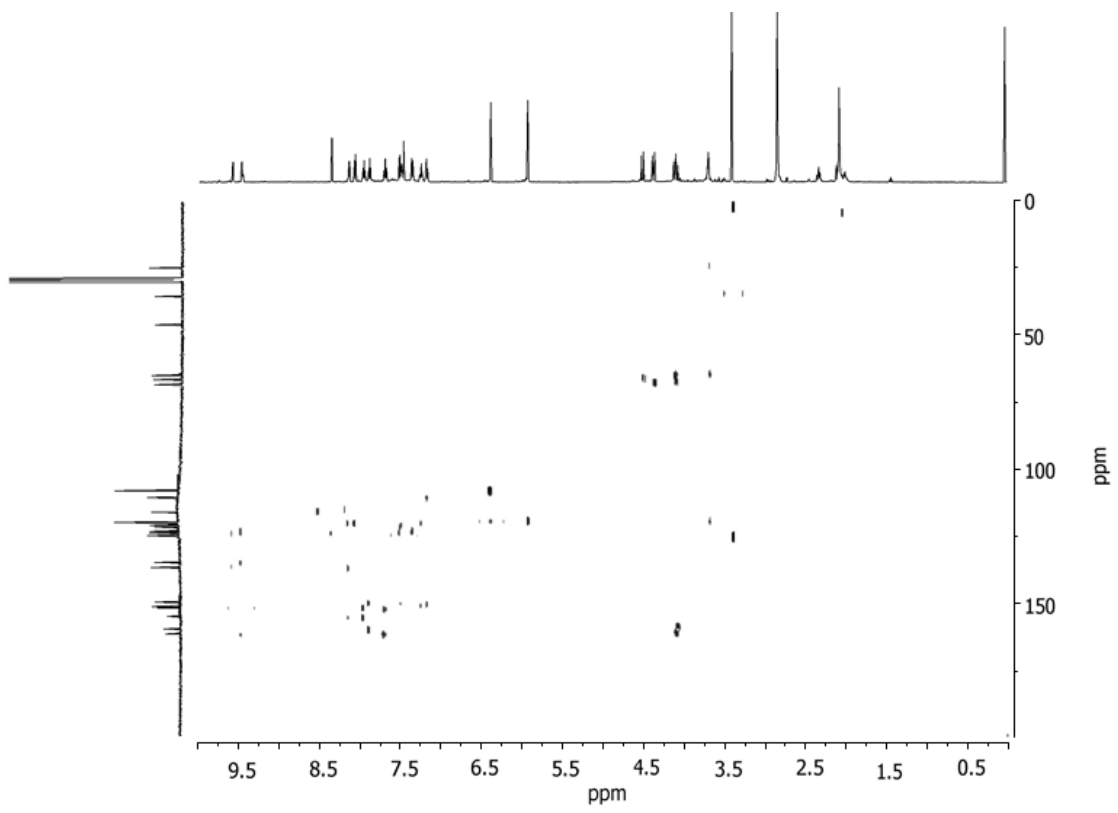
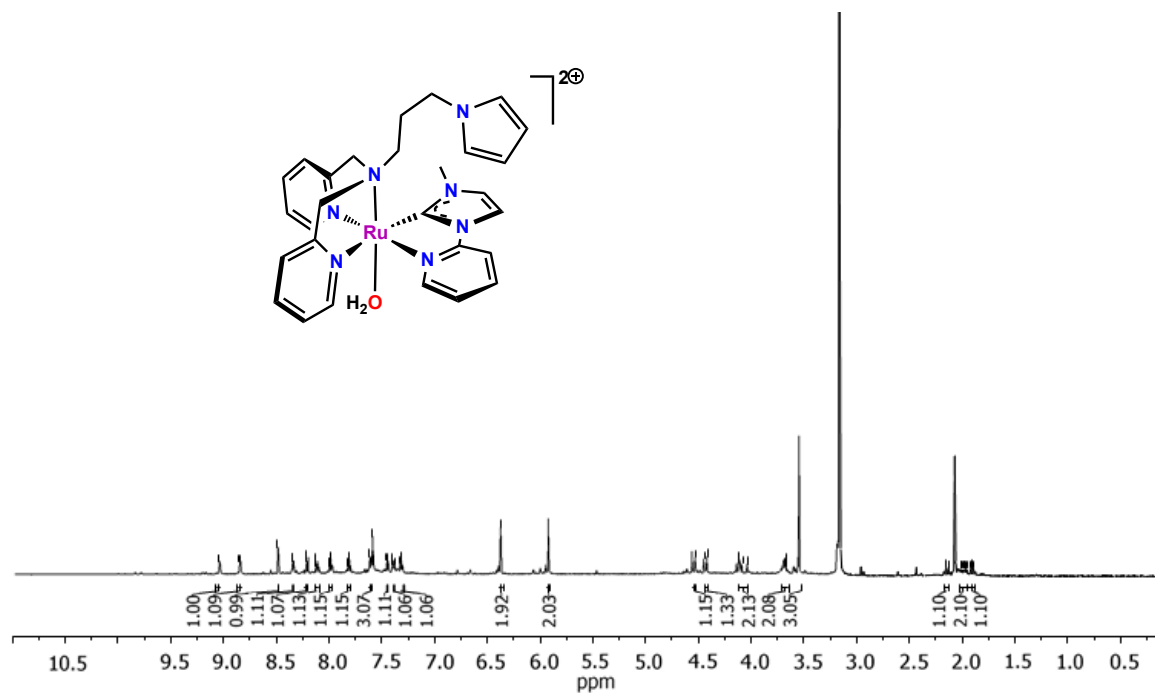
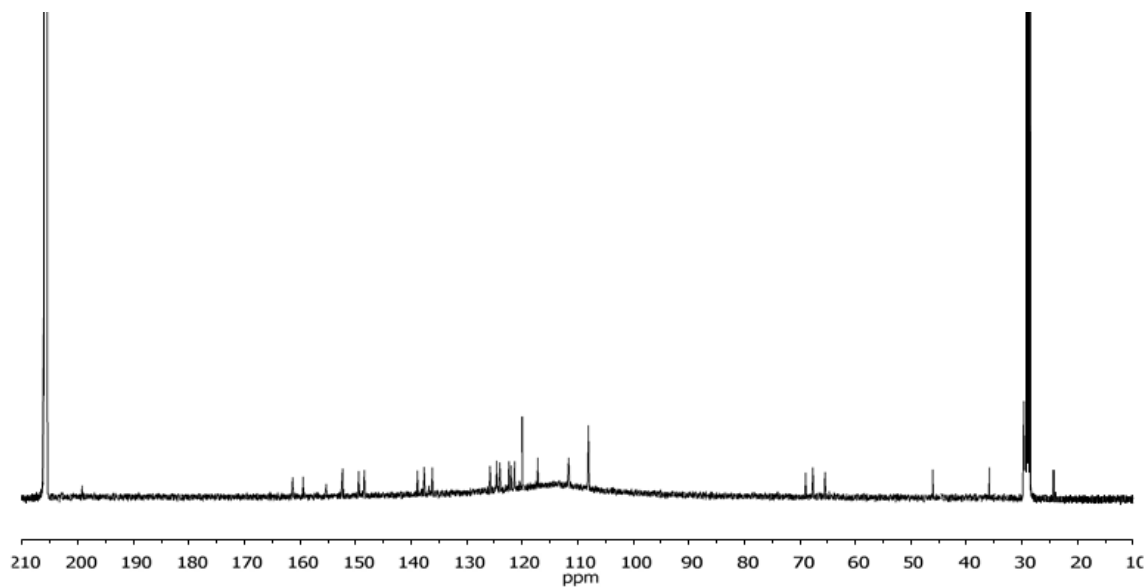


Figure S 5. NMR spectra (600 MHz, 298 K, d_6 -acetone) *trans, fac*-[Ru^{II}(CN-Me)(bpea-pyr)(H₂O)]²⁺, **4**: (a) ¹H-NMR, (b) ¹³C-NMR, (c) COSY, (d) NOESY, (e) HSQC, (f) HMBC.

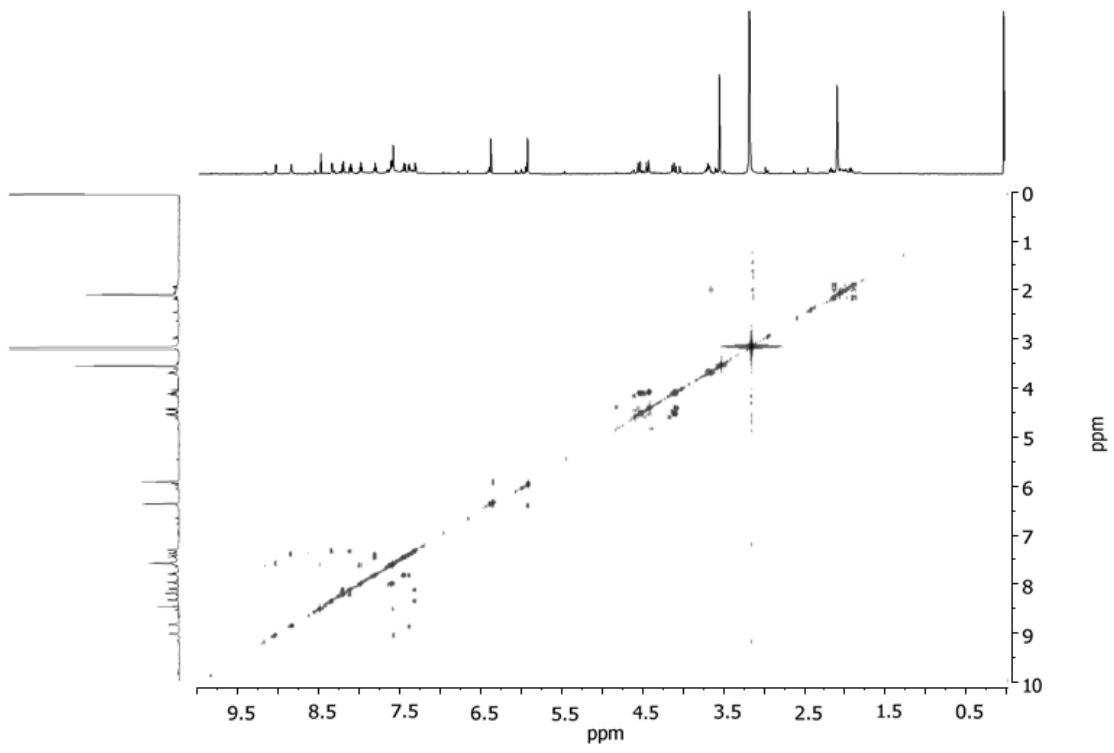
(a)



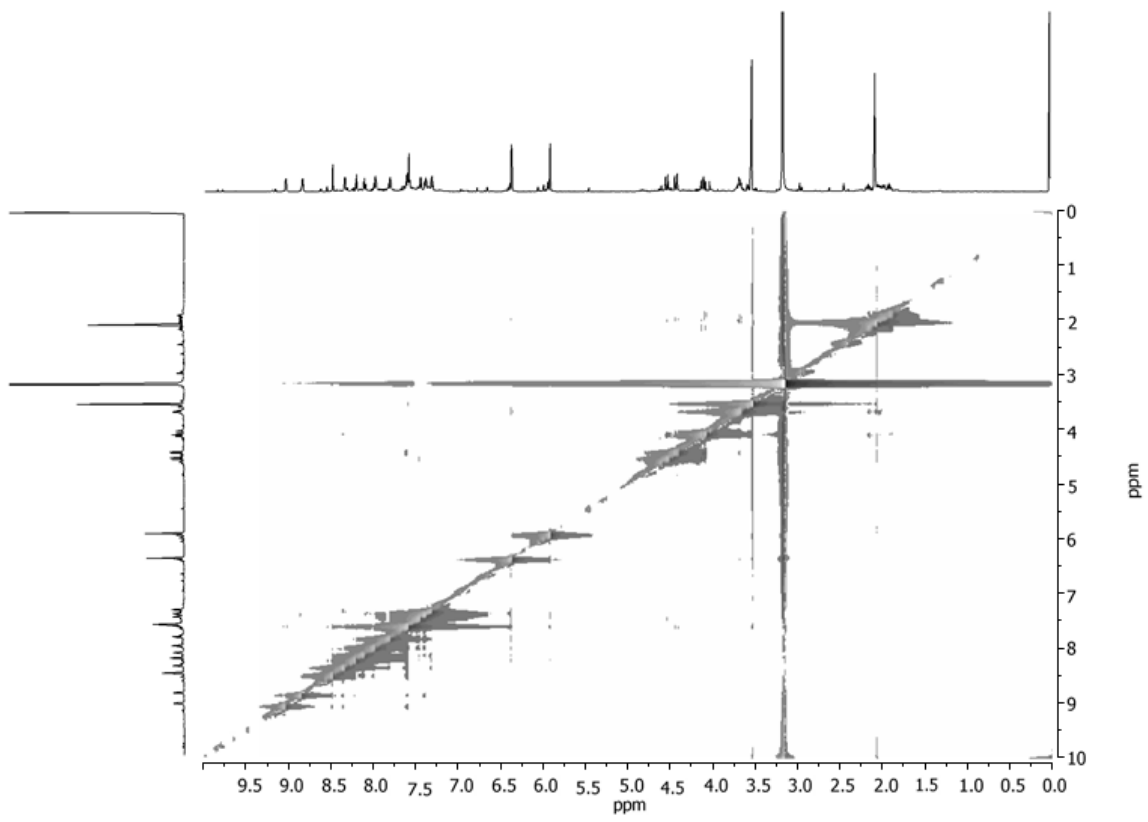
(b)



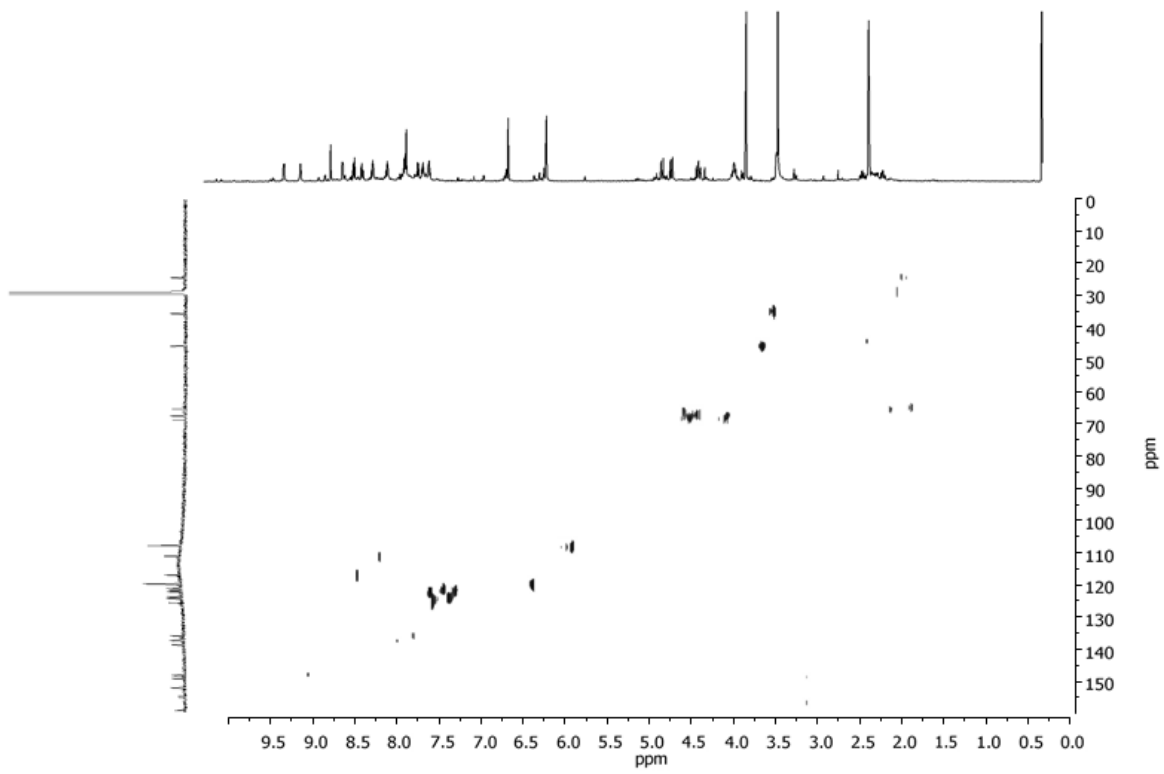
(c)



(d)



(e)



(f)

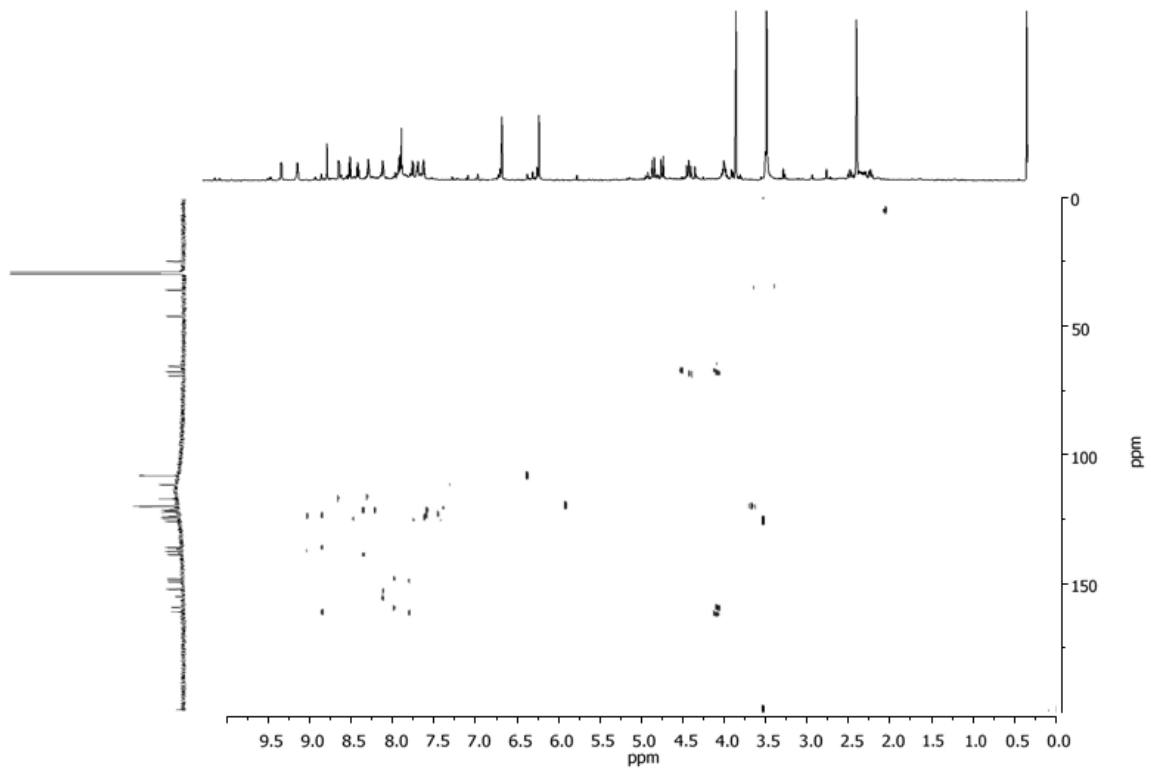


Figure S 6. Cyclic voltammogram of complex 3 (1 mM) registered in CH₂Cl₂ + 0.1 M TBAH at a glassy carbon disk electrode (scan rate = 100 mV s⁻¹).

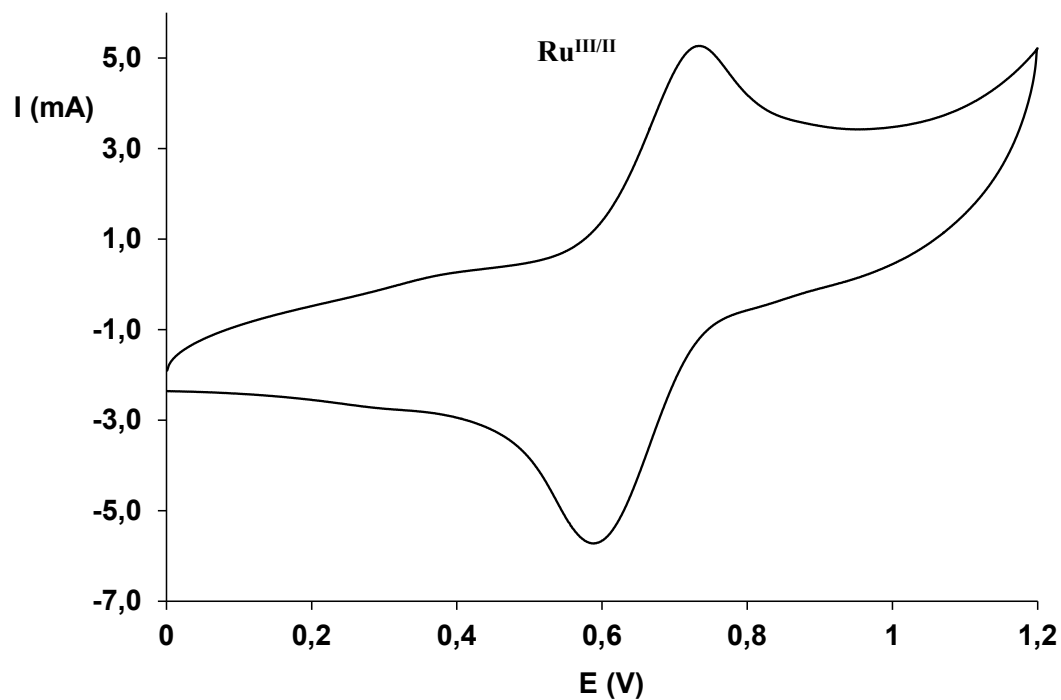


Figure S 7. Cyclic voltammogram of complex 4 (1 mM) in CH₂Cl₂ + 0.1 M TBAH at a glassy carbon disk electrode (scan rate = 100 mV s⁻¹).

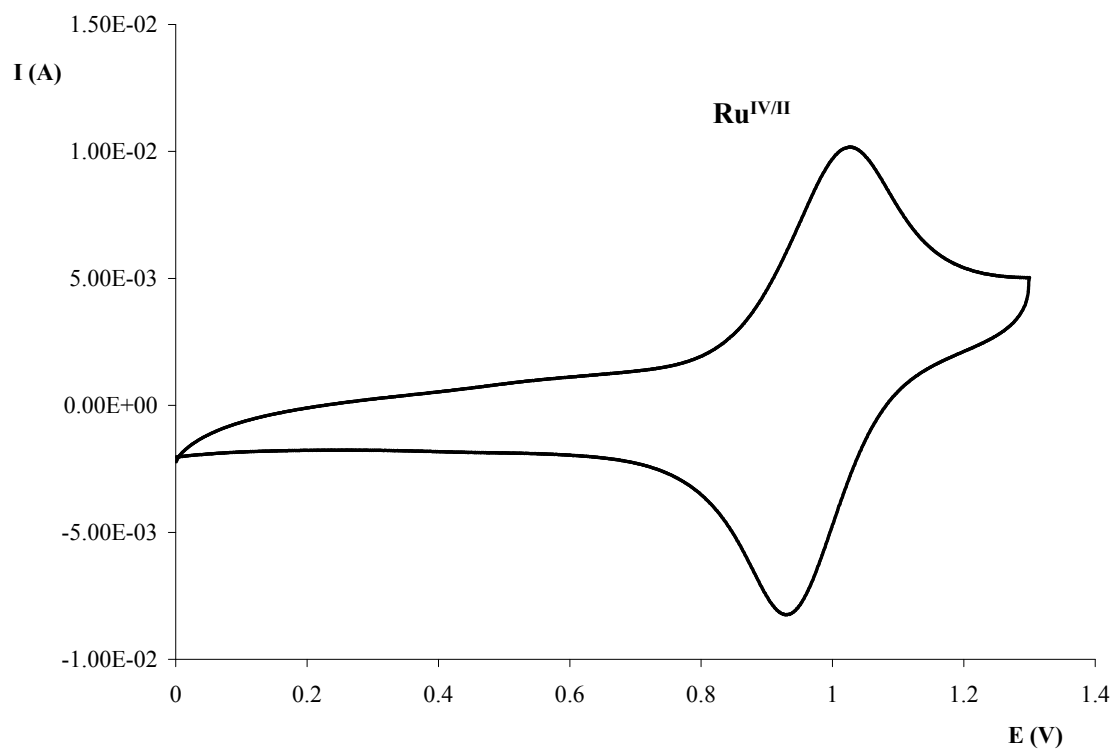


Figure S 8. (a) Growing of a **C/poly-3** film in $\text{CH}_2\text{Cl}_2 + 0.1 \text{ M TBAH}$ at a glassy carbon disk electrode (diameter = 3 mm) by scanning the potential between 0 and 1.3 V throughout 30 cycles (scan rate = 100 mV s^{-1}). (b) Cyclic voltammograms registered after transferring the **C/poly-3** modified electrode into a blank electrolyte solution (5 cycles were registered; final amount of anchored complex = $4.36 \cdot 10^{-10} \text{ mols} \cdot \text{cm}^{-2}$).

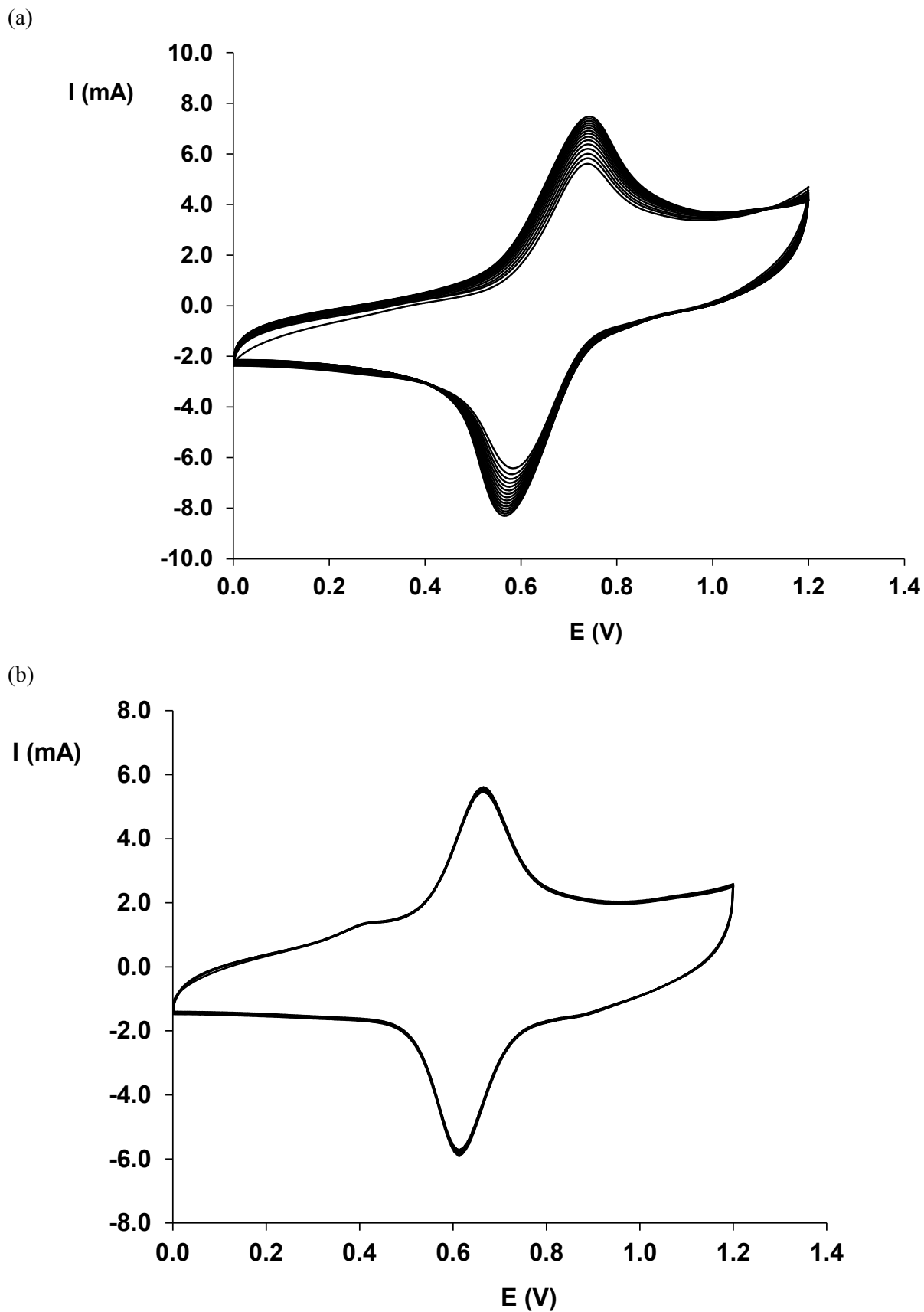


Figure S 9. Linear regression of $E_{1/2}$ values vs. pH for the cyclic voltammograms of complex **4** registered in aqueous media.

